Characterization of the Primary Photointermediates of *Drosophila* Rhodopsin†

Bryan W. Vought,‡,§ Ernesto Salcedo,||,⊥ Linda V. Chadwell,|| Steven G. Britt,||,⊥ Robert R. Birge,*,‡,▽ and Barry E. Knox*,○

Departments of Chemistry and Biology, Syracuse University, 111 College Place, Syracuse, New York 13244-4100, Institute of Biotechnology and Department of Molecular Medicine, The University of Texas Health Science Center, San Antonio, Texas 78245, and Department of Biochemistry and Molecular Biology, SUNY Health Science Center, 750 East Adams Street, Syracuse, New York 13210

Received May 18, 2000; Revised Manuscript Received July 14, 2000

ABSTRACT: Invertebrate opsins are unique among the visual pigments because the light-activated conformation, metarhodopsin, is stable following exposure to light in vivo. Recovery of the light-activated pigment to the dark conformation (or resting state) occurs either thermally or photochemically. There is no evidence to suggest that the chromophore becomes detached from the protein during any stage in the formation or recovery processes. Biochemical and structural studies of invertebrate opsins have been limited by the inability to express and purify rhodopsins for structure−function studies. In this study, we used *Drosophila* to produce an epitope-tagged opsin, *Rh1-1D4*, in quantities suitable for spectroscopic and photochemical characterization. When expressed in *Drosophila*, *Rh1-1D4* is localized to the rhabdomere membranes, has the same spectral properties in vivo as wild-type Rh1, and activates the phototransduction cascade in a normal manner. Purified *Rh1-1D4* visual pigment has an absorption maximum of the dark-adapted state of 474 nm, while the metarhodopsin absorption maximum is 572 nm. However, the metarhodopsin state is not stable as purified in dodecyl maltoside but decays with kinetics that require a double-exponential fit having lifetimes of 280 and 2700 s. We investigated the primary properties of the pigment at low temperature. At 70 K, the pigment undergoes a temperature-induced red shift to 486 nm. Upon illumination with 435 nm light, a photostationary state mixture is formed consisting of bathorhodopsin ($\lambda_{max} = 545$ nm) and isorhodopsin ($\lambda_{max} = 462$ nm). We also compared the spectroscopic and photochemical properties of this pigment with other vertebrate pigments. We conclude that the binding site of *Drosophila* rhodopsin is similar to that of bovine rhodopsin and is characterized by a protonated Schiff base chromophore stabilized via a single negatively charged counterion.

Visual pigments are composed of an 11-*cis*-retinal-based chromophore covalently attached via a Schiff base linkage to an apoprotein (*1*). Light induces the isomerization of 11-*cis*-retinal to *all-trans*-retinal (the primary event), initiating conformational changes that produce a form of the protein that activates a G protein signaling system (*2*, *3*). Bovine rhodopsin has a neutral retinal binding pocket, with a single glutamate residue (counterion) neutralizing the charge from the protonated Schiff base linkage (*4*−*7*). The active form of rhodopsin is not thermally stable and undergoes facile hydrolysis of the Schiff base linkage with retinal, resulting in free *all-trans*-retinal and apoprotein.

In contrast to the vertebrate rhodopsins, little is known about the protein−chromophore interactions in the invertebrate opsins. The observation of spectroscopic, photochemical, and primary counterion differences between the invertebrate and vertebrate pigments suggests that the binding sites of the two opsins are quite different. Some of the key differences are presented in Table 1. Invertebrate opsins are unique among visual pigments because the activating state is stable and can be converted thermally or photolytically back to the original form (*8*−*12*). Sequence comparisons between vertebrate rod and invertebrate opsins indicate only about 30% amino acid identity between the two protein classes. In fact, it is unclear what the overall charge of the invertebrate retinal binding site is because there is usually a tyrosine or phenylalanine at the vertebrate counterion position. Resonance Raman results suggest that the tyrosine at this position is not ionized in octopus rhodopsin (*13*), even though the Schiff base linkage is protonated (*14*−*16*). Most of the invertebrate biochemistry is based on cephalopod opsins because they can be purified in quantities suitable for biophysical experiments. The cephalopod opsins have been studied by low-temperature and time-resolved spectroscopies, as well as with chromophore analogues (e.g., refs

† This work was supported in part by NIH Grants GM 34548 (R.R.B.), EY 11256 (B.E.K.), and EY10759 (S.G.B.) and by the W. M. Keck Foundation.

* Address correspondence to either author: R.R.B., phone 860-486-6720, fax 860-486-2981, e-mail rbirge@syr.edu; B.E.K., phone 315-464-8719, fax 315-464-8750, e-mail knoxb@hscsyr.edu).

‡ Syracuse University.

§ Present address: Department of Biological Chemistry and Molecular Pharmacology, Harvard Medical School, 240 Longwood Ave., Boston, MA 02115.

|| The University of Texas Health Science Center.

⊥ Present address: Departments of Cellular and Structural Biology and Ophthalmology, University of Colorado Health Sciences Center, 4200 East 9th Ave., Box B111, Denver, CO, 80262.

▽ Present address: Departments of Chemistry & Molecular and Cell Biology, 55 North Eagleville Rd., University of Connecticut, Storrs, CT 06269.

○ SUNY Health Science Center.

10.1021/bi001135k CCC: $19.00
Published on Web 10/26/2000

Table 1: Comparison of Vertebrate and Invertebrate Pigments

	bovine rhodopsin	*Drosophila*
pigment		
native retinal	A_1	3-hydroxyretinal
counterion	Glu	Tyr?
batho		
spectral shift	red	red
energy storage	135 kJ/mol	?
quantum efficiency	0.65	?
activating form		
chromophore Schiff base linkage	unprotonated	protonated
stability *in vitro*	unstable	unstable
stability *in vivo*	unstable	stable
photostationary states at 70 K		
effect of red light	mostly 9-cis	mostly 9-cis
effect of blue light	50−70% all-trans	>90% all-trans
ΔE (batho − initial state) (cm^{-1})	1600	2200
ΔE [(9-cis) − initial state] (cm^{-1})	800	1100

17−*25*). These studies have suggested that the photochemistry of invertebrate opsins is simpler than for vertebrate opsins. After isomerization, vertebrate opsins require the deprotonation of the Schiff base, as well as protonation of the counterion to activate the G protein (*26*). Because the "counterion" is presumed to be absent in invertebrate opsins, only isomerization appears to be required for activation (*27*).

Cephalopods are not useful for genetic or site-directed mutagenesis studies. Moreover, there are currently no heterologous systems for producing functional invertebrate opsins that are comparable to those available for vertebrate opsins (*28*). *Drosophila* offers great potential for visual pigment studies, since the fly can be genetically manipulated and produced in large quantities. The most abundant rhodopsin from *Drosophila*, rhodopsin 1 (also referred to as *Rh1* and *ninaE*) has a maximum absorption of ~480 nm and a stable metarhodopsin with an absorption maximum ~570 nm, when studied in rhabdomere extracts (*29*−*31*). The *Rh1* chromophore, 3-hydroxy-11-*cis*-retinal (*32*, *33*), is only believed to blue-shift the absorption maximum of the opsin compared to the vitamin A_1-derived retinal, not to cause any functional differences. Previous studies have raised as many questions as they have answered. What is the charge of the retinal binding pocket in invertebrate opsins? How can there be no counterion present in a hydrophobic, membrane-bound protein? Are the mechanisms of spectral tuning in invertebrate opsins and vertebrate opsins identical? Ultimately, what role do the electrostatics of the binding pocket play in the bistability of invertebrate opsins?

In this study, we have introduced a gene encoding an epitope-tagged *Rh1* (*Rh1-1D4*)[1] into *ninaE* mutant flies in which the endogenous *Rh1* gene has been deleted (*34*, *35*). The expression of *Rh1-1D4* in the native photoreceptor cells provides the proper environment for the biosynthesis and folding of the visual pigment. In addition, the epitope tag permits the one-step immunoaffinity purification of the expressed visual pigment. We have obtained quantities of purified *Rh1-1D4* opsin suitable for spectroscopic investigations and studied its photochemistry. Purified *Rh1-1D4* in delipidated form converts to a stable metarhodopsin at 4 °C, but at 20 °C metarhodopsin decays, likely forming free retinal and opsin. Furthermore, we were able to trap the bathointermediate of rhodopsin at 70 K. By analyzing the bathochromic intermediate of *Rh1-1D4*, we conclude that the binding site is electrostatically similar to bovine rhodopsin with a counterion stabilizing a protonated Schiff base−retinal linkage. The approach used in these studies is readily adaptable to the expression of site-specific mutants or chimerics for structure−function studies of other invertebrate opsins.

MATERIALS AND METHODS

Expression of the Epitope-Tagged Form of the Rh1 Opsin in Transgenic Drosophila. An epitope-tagged form of the *Rh1* gene (referred to as *Rh1-1D4*) was made by replacing the region encoding the last 14 amino acids of *Rh1* with the sequence encoding amino acids 335−348 of bovine rhodopsin (*36*). This region corresponds to the epitope recognized by the 1D4 monoclonal antibody (*37*). This construct was generated within a 5.4 kb *Rh1* genomic fragment that contains the entire *Rh1* coding region, 2.5 kb of promoter, the native transcription start site, and 5′- and 3′-untranslated regions. This construct would therefore drive the expression of *Rh1-1D4* in the R1-6 photoreceptors where the wild-type protein is normally expressed. The construct was subcloned into the y^+-marked P-element vector C4 and injected into *y w; sr ninaE*^{17} mutant embryos, as previously described (*38*). Multiple independent P-element-mediated germline transformants were obtained by standard techniques (*39*). The strains used in this study were constructed with visible markers and balancer chromosomes and were maintained on standard cornmeal/yeast extract/molasses/agar food in humidified incubators at 25 °C on a 12 h light/dark cycle.

Microscopy. The immunohistochemistry and confocal imaging were performed as previously described (*38*), with monoclonal 1D4 antibody (*37*). Secondary antibodies and other immunological reagents were obtained from Jackson ImmunoResearch Laboratories, Inc. (West Grove, PA). The specimens were incubated with the primary antibody at 4 °C overnight (or at room temperature for 1.5 h), and the incubations with the secondary antibody were performed at

[1] Abbreviations: *Rh1-1D4*, epitope-tagged *Drosophila* Rh1 opsin; DTT, dithiothreitol; HEPES, *N*-(2-hydroxyethyl)piperazine-*N*′-2-ethanesulfonic acid; LM, *N*-dodecyl β-D-maltoside; MOPS, 4-morpholinepropanesulfonic acid; PSS*xyz*, photostationary state generated at wavelength *xyz* nm; WT, wild type.

room temperature for 1 h. The confocal image was collected with a Zeiss LSM-310 (Thornwood, NY).

Electrophysiology, Microspectrophotometry, and Spectral Sensitivity Analysis. Electroretinogram (ERG) recordings were obtained from immobilized white-eyed (*w*) flies by use of glass microelectrodes filled with normal saline [0.9% NaCl (w/v)] as previously described (*38*, *40*). Microspectrophotometry was performed as previously described (*31*). Spectral sensitivity was measured by a modification of the voltage-clamp method of Franceschini (*41*, *42*), which we have described in detail elsewhere (*31*, *40*). Briefly, the amplitude of the ERG response to a flickering (10 Hz) monochromatic stimulus was maintained at a criterion level while the wavelength of stimulating light was varied during a scan. Throughout the scan, the criterion response was maintained by constantly adjusting the light intensity with a proportional-integral-derivative algorithm (*43*). Spectral sensitivity (SS) was defined as the inverse of the light flux (number of photons) required to produce the criterion response. This is proportional to the inverse of the product of the light intensity times the wavelength [i.e., SS $\propto$ 1/(light intensity (microwatts per square centimeter) $\times$ wavelength)]. Sensitivity data were normalized to an amplitude of 1.0 at the wavelength of maximal sensitivity, averaged, and smoothed with a window of 10 nm.

Purification of Rh1 Rhodopsin from Drosophila. The purification methods used here are similar to the reported procedures of Kiselev and Subramaniam (*44*, *45*). Unless otherwise stated, all of the following procedures were carried out at 4 °C and in the dark or deep red light (Kodak no. 2). *Drosophila* were kept in the dark 24 h prior to harvesting and then collected and frozen in liquid nitrogen. The frozen animals were vortexed in 50 mL conical tubes to sever the heads, bodies, and appendages, which were separated and collected in chilled, stainless steel sieves. Heads (7 mL) were homogenized with a motorized Teflon homogenizer in 250 mL of buffer A [250 mM sucrose, 120 mM KCl, 10 mM MOPS (pH 6.7), 5 mM $MgCl_2$, 1 mM DTT, 10 μg/mL leupeptin, and 1.2 μg/mL pepstatin]. The homogenate was centrifuged twice at 1000*g* for 5 min at 4 °C to remove the insoluble tissue. The supernatant, containing photoreceptor membranes, was collected by ultracentrifugation at 45000*g* for 1 h at 4 °C. The membrane pellet was homogenized with a Brinkman polytron in 90 mL of buffer A containing 1% *N*-dodecyl β-D-maltoside (LM) and slowly mixed for 10 h. The insoluble material was separated by centrifuging twice at 45000*g* for 20 min and saved for a protein gel. The *Rh1-1D4* rhodopsin was then purified by immunoaffinity chromatography (*28*). Briefly, the supernatant was slowly mixed with 1.6 mL of packed 1D4-Sepharose beads (2 mg of IgG/mL) for 4 h. 1D4 IgG was obtained from the Cell Culture Center and National Center for Research Resources (Minneapolis, MN). The 1D4−Sepharose beads were then washed with 300 mL of wash buffer [20% glycerol, 120 mM KCl, 5 mM $MgCl_2$, 50 mM HEPES (pH 6.6), and 0.1% LM]. The protein was eluted with 40 μM competing peptide in wash buffer and concentrated in a C-30 Centricon tube (Amicon). The yield was approximately 215 μg of *Rh1-1D4* rhodopsin from 7 mL of fly heads (1 mL $\sim$ 1000 heads). Western blots were performed as previously described (*46*). Opsin was detected with the 1D4 IgG and arrestins with a mixture of two antibodies to each of the two *Drosophila* arrestin proteins [Arr1 and Arr2 (*47*)].

Formation of Rh1 Metarhodopsin. A Cary 300 spectrophotometer (Varian Inc.) was used with a circulating water bath to control the sample temperature, which was monitored in the cuvette by a thermocouple connected to a Stanford Research Systems SR630 thermocouple monitor. Photoconversion was performed with a 250 W quartz halogen lamp with the appropriate interference filter (either 03FIV105 or 03FIV115 (Melles Griot), for maximum transmission = 461 $\pm$ 5 nm or 562 $\pm$ 5 nm, respectively).

Cryogenic Spectroscopy and Photochemistry of Rh1. We modified our Air Products Displex helium refrigerator cold tip so that a small-volume sample cell could be used and inserted coupling optics into our Shimadzu UV−Vis−NIR 3101 spectrophotometer to maximize light throughput (*48*). Photoconversion of the pigments was performed by use of an Nd:YAG-pumped optical parametric oscillator with amplifier (Infinity with internal XPO, Coherent Inc.). Coupling optics maximized illumination of the sample while in the cold tip. Protein samples contained 67% glycerol and 0.05% LM in wash buffer. The samples were thermally equilibrated at 70 K for 1 h and then illuminated with blue light relative to the absorption maximum (435 nm) to generate a photostationary state containing a maximum amount of the bathochromic photoproduct. Subsequently, red light relative to the absorption maximum (550 nm) was used to generate the reverse photostationary state. The methods and procedures of generating and characterizing the photostationary states have been reported previously (*48*).

RESULTS AND DISCUSSION

Expression of the Rh1-1D4 opsin in the R1-6 cells of Drosophila. We expressed an epitope tagged form of the *Rh1* opsin (*Rh1-1D4*) in the R1-6 photoreceptor cells of *Drosophila* under the control of the *ninaE* opsin gene promoter. The R1-6 photoreceptor cells are a suitable environment for the expression of novel opsins and have been used extensively for studying the spectral and physiological properties of novel or modified opsin genes in vivo, including those from other invertebrates (*31*, *40*, *49*−*51*).

Transgenic flies expressing the epitope-tagged *Rh1-1D4* opsin construct showed proper localization of the tagged protein to the rhabdomeres of the R1-6 cells of the compound eye (Figure 1A). This demonstrates that the transgene is expressed in the expected cell types and that the protein is stable and appropriately targeted within the photoreceptor cells. A similar 1D4 epitope tagged form of Rh1 has been shown to be normally processed and localized within the *Drosophila* R1-6 cells.[2] The *Rh1-1D4* protein bound retinal and produced a visual pigment with absorption properties characteristic of the wild-type pigment. Using in vivo microspectroscopy (MSP, Figure 1B), we found that the difference spectra of *Rh1-1D4* and the native pigment were identical. To assess the functional activity of the *Rh1-1D4* opsin, we examined the electroretinograms of transgenic flies. *ninaE* flies were used as a host strain because they lack the visual pigment normally expressed in the R1-6 photoreceptor

[2] Webel, R., Menon, I., O'Tousa, J. and Colley, N. (2000) *J. Biol. Chem. 275*, 24752−24759.

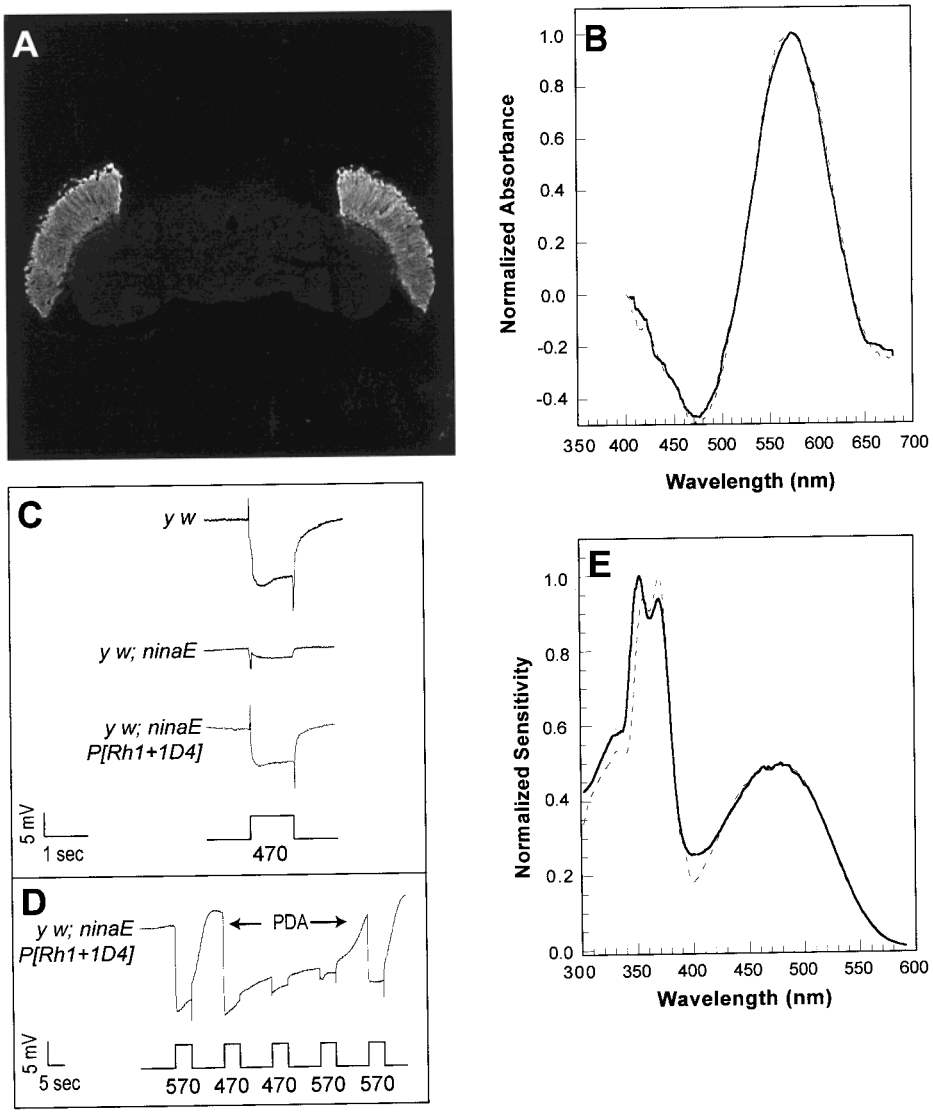

FIGURE 1: Expression and function of *Rh1-1D4* in *Drosophila*. (A) Confocal image showing the immunolocalization of the *Rh1-1D4* protein in transgenic flies. The protein is expressed by the R1-6 cells and is localized in the rhabdomeres of these cells. (B) Rhodopsin/metarhodopsin difference spectra measured in vivo by microspectrophotometry. The difference spectra measured from control flies (*y w*, dashed line, $n = 2$) is virtually identical to that measured from transgenic flies expressing the *Rh1-1D4* construct (*y w*; *ninaE P[Rh1-1D4]*, solid line, $n = 2$). The difference spectra were measured and calculated as described previously (*31*) using adapting lights (λ_1 and λ_2) of 475 and 580 nm (respectively) for both strains of flies. The *y w*; *ninaE* host strain, which lacks the Rh1 opsin, does not have a detectable difference spectrum (data not shown). The averaged spectra were filtered (removing data points with an error > 30% within a 10 nm window), and the resulting spectra were then smoothed by a running average over a 10 nm window. The baseline of the spectra for the control and transgenic flies were offset by −0.1 and −0.195, respectively, and normalized to 1.0. (C) Electroretinograms recorded from control (*y w*, top trace), mutant host strain (*y w*; *ninaE*, middle trace), and *Rh1-1D4* transgenic flies (lower trace). Control flies display a robust light-induced depolarization that is maintained during the stimulus. The mutant host strain (*y w*; *ninaE*) has a dramatically reduced response to light due to the loss of the Rh1 opsin normally expressed in the R1-6 cells. The small residual response is due to the R7 and R8 cells, which are unaffected by the mutation. When the *Rh1-1D4* transgene is introduced into this host strain, the light response is restored. This demonstrates that the *Rh1-1D4* pigment is biologically active and is capable of coupling to the downstream components of the phototransduction cascade in a normal manner. (D) Prolonged depolarizing afterpotential (PDA) in flies expressing the *Rh1-1D4* pigment. A PDA is only generated when a substantial amount of rhodopsin has been photoconverted to metarhodopsin, and the wavelengths at which the PDA can be induced and terminated (470 and 570 nm used in this experiment, respectively) are dependent on the absorption properties of rhodopsin and metarhodopsin (discussed in ref *31*). This demonstrates that rhodopsin and metarhodopsin can be photoconverted with appropriate wavelengths of light, and that the *Rh1-1D4* metarhodopsin is stable and active in vivo, because of its ability to maintain a depolarization after the stimulus has ended. Light pulses in panel C were attenuated 3 log units (0.6 mW/cm^2) while those in panel D were unattenuated and correspond to 0.50 mW/ cm^2 at 470 nm and 0.35 mW/cm^2 at 570 nm. The wavelengths of stimulating light are indicated under the stimulus trace. Panel E shows the spectral sensitivity profiles of control flies (*y w*, dashed line, $n = 2$) and transgenic flies expressing the *Rh1-1D4* construct (*y w*; *ninaE P[Rh1-1D4]*, solid line, $n = 5$). The spectral sensitivities of the two strains are virtually identical. Both strains show prominent peaks of sensitivity in the UV region (near 330, 355, and 370 nm) that are due to the effect of the sensitizing pigment, and both also show a broad peak in the blue region ($\lambda_{max} = 478$ nm) that corresponds to the absorption profile of the Rh1 rhodopsin. The *y w*; *ninaE* host strain does not have a detectable spectral sensitivity when measured by this recording paradigm, because the amplitude of the response is insufficient to meet the criterion level as described under Materials and Methods. Thus the small contribution of the R7 and R8 cells present in the *y w*; *ninaE* host strain would not be expected to significantly interfere with the measurement. Sensitivity values were averaged, and those exceeding 30% error within a window of 10 nm were filtered out. The resulting spectra were then smoothed with a window of 10 nm and normalized to an amplitude of 1.0.

cells. Figure 1C shows responses to 470 nm light in control (*y w*, top trace) and y w; *ninaE* mutant flies (middle trace). The *ninaE* mutants exhibit only a small response from the R7 and R8 cells, which are not affected by the *ninaE* mutation. When the *Rh1-1D4* opsin construct was introduced into the *y w*; *ninaE* background (bottom trace), the electrophysiological response to light was restored. The *Rh1-1D4* flies also exhibited a prolonged depolarizing afterpotential (PDA) following stimulation with 470 nm light (Figure 1D). The PDA occurs after a substantial amount of the rhodopsin is converted to a stable metarhodopsin form (*10*). The PDA can be terminated by photoconverting metarhodopsin back to the rhodopsin form with 570 nm illumination (Figure 1D). These results demonstrate that the epitope-tagged form of the Rh1 protein is biologically active and has functional properties that are equivalent to the wild-type pigment.

To determine the spectral sensitivity of the *Rh1-1D4* rhodopsin, we measured spectral sensitivity physiologically in transgenic flies that expressed the epitope-tagged form of the pigment. As shown in Figure 1E, the flies are sensitive to light in the blue-green region of the spectrum. The sensitivity curve in the visible region is well fit by a rhodopsin absorption nomogram having a λ_{max} at 478 nm [determined as described previously (*31*, *40*, *49*−*51*)]. Moreover, the photoreceptors in *Rh1-1D4* flies exhibit sensitivity to UV light (Figure 1E), demonstrating that *Rh1-1D4* efficiently couples to the sensitizing pigment (*52*, *53*). Apparently, the alteration at the carboxyl terminus does not affect the presumed binding site for the sensitizing pigment.

Purification of Rh1-1D4 from Drosophila. The epitope tag on *Rh1* permitted the purification of the visual pigment in delipidated form. The absorbance maximum of the pigment was 474 nm with a full width of 4700 cm^{-1} (Figure 2, curve 1), in good agreement with the in vivo measurements (Figure 1B,E) and previous reports on light−dark difference spectra of rhabdomere membranes (*30*, *45*, *54*). A western blot of the purified *Rh1-1D4* showed a diffusely migrating band of ~36 kDa when probed with 1D4 antibody (Figure 3, left panel). There was no copurifying arrestin in the preparation (Figure 3, right panel). We obtained ~30 μg of pigment/mL of heads, which translates to approximately 30 ng of opsin/fly.

In addition to the opsin absorption at 280 nm and the retinal absorption at 474 nm, we observed three sharp absorption bands in the UV region (337, 355, and 375 nm), the same peaks found in spectral sensitivity measurements (see Figure 1E). Since the material remains associated with the protein through extensive washing in detergent solution and has the same UV absorption profile as found in the in vivo measurements, we believe that the sensitizing pigment may form a stable complex with *Rh1-1D4*. Either the pigment is covalently attached to the opsin or there may be a high-affinity interaction between the pigment and the opsin. Our results do not permit a distinction between these alternatives. Furthermore, the identity of the pigment is not clear from the spectrum alone. From the UV absorbance properties, it appears to be a retinyl polyene with five conjugated double bonds that is present in significant amounts relative to the principal chromophore, 3-hydroxyretinal. *Drosophila* heads contain substantial amounts of 3-hydroxyretinol (*55*), previously proposed as the sensitizing pigment (*33*). However in ethanol, 3-hydroxyretinol has a single, inhomogeneously broadened absorption maximum ~320 nm (*33*). When retinol binds noncovalently to bacterio-opsin (*56*) or cellular retinol

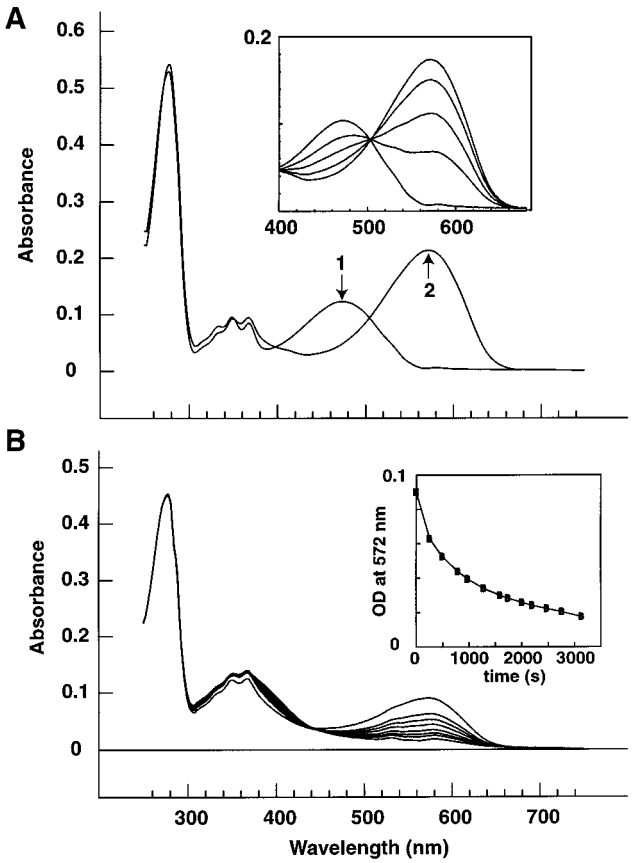

FIGURE 2: (A) UV−visible spectra of *Drosophila* rhodopsin *Rh1-1D4* and metarhodopsin at 4 °C. The pigment has an absorption maximum of 474 nm before illumination (curve 1). Upon illumination with blue light (461 nm), the absorption maximum shifts to 572 nm (curve 2). At 4 °C, metarhodopsin is stable. (Inset) Illumination with 562 nm light converts the metarhodopsin to the original (preilluminated) spectrum. The inset shows the isosbestic point at 502 nm during photoconversion. (B) Decay of metarhodopsin at 20 °C. The inset shows a double-exponential fit to the absorption decrease at 572 nm due to decay of metarhodopsin. The decay curve corresponds to lifetimes of 280 and 2700 s.

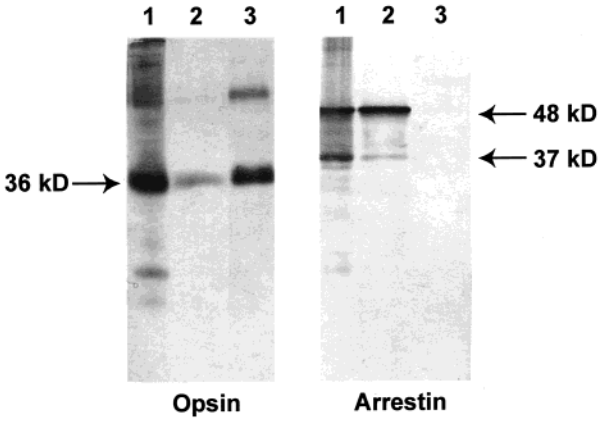

FIGURE 3: Western blot analysis of purified *Rh1-1D4*. Various fractions from the purification, corresponding to ~10 heads, were solubilized in 1% SDS and analyzed by western blots. The primary antibody was either 1D4 (left panel) or a mixture of anti-arrestin antibodies (right panel). Lane 1 contained rhabdomere membranes, lane 2 contained material not bound to 1D4-Sepharose, and lane 3 contained the material eluted by the competing peptide. Sizes were determined by comparison to prestained molecular weight standards.

binding protein (*57*), absorption maxima of 343, 357, and 377 nm or 334, 348, and 366 nm are observed, respectively. The discrepancy between the solution and protein-associated forms of retinol can be explained by assuming that the shift in λ_{max} and fine structure arises from the coplanarity of the β-ionone with the polyene chain (*33*), as has been observed with retinol model compounds (*58*). The UV spectrum of *Rh1-1D4* (λ_{max} 337, 355, and 375 nm) is also consistent with a number of other related compounds (*59*), including retroretinyl aldehyde, alcohol, or fatty acid esters. At present, the vibronic spectra are not resolved sufficiently to permit discrimination between the various alternatives. We are currently investigating the origin and photochemical properties of the copurifying UV-absorbing pigment.

Spectrum of Rh1 Metarhodopsin. Previous studies of membrane and micellar extracts from *Drosophila* have suggested that the behavior of *Rh1* metarhodopsin is dependent on the presence of arrestin (*44*, *45*, *54*). In dark-adapted membranes with arrestin present, the lifetime of metarhodopsin appears extended. Thus, a second photon of light is able to convert metarhodopsin back to the original pigment, like other bistable invertebrate opsins (*8*, *10*, *11*, *60*). In washed membranes in which arrestin has been depleted, metarhodopsin does not revert to the original state but undergoes hydrolysis of the Schiff base linkage, as in most vertebrate opsins. To determine the stability of purified metarhodopsin, we trapped it at reduced temperature. *Drosophila Rh1-1D4* was equilibrated in the spectrometer at 4 °C for 1 h (Figure 2A, curve 1) and then illuminated with 460 nm light. The absorption maximum shifted to 572 nm (Figure 2A, curve 2). This absorption maximum is in reasonable agreement with literature values for the absorption of metarhodopsin at ~580 nm (*29*, *54*). When trapped at 4 °C, metarhodopsin is stable and photoreversible to the original spectrum with 565 nm light (Figure 2A, inset). Metarhodopsin, however, was not stable at 20 °C. The absorption at 572 nm show a time-dependent decrease with a concomitant increase in absorption at ~380 nm (Figure 2B). The decay of metarhodopsin required a double-exponential fit, with lifetimes of 280 and 2700 s (Figure 2B, inset).

The experiments presented here show that the purified *Rh1-1D4* does not form a stable metarhodopsin species at room temperature. This may be due to the absence of arrestin (*54*) in the purified preparation (Figure 2). Alternatively, it may be that the conditions used to isolate and study the protein, 0.1% dodecyl maltoside and the delipidating purification, are inappropriate conditions for stability of the metarhodopsin conformation. Both invertebrate and vertebrate opsins are very sensitive to detergent and lipid environment (e.g., refs *45* and *61*−*66*). However, since extracts of rhabdomere membranes, under different conditions (1% CHAPS/1% dimyristoylphosphatidylcholine or reconstituted liposomes), showed essentially the same lack of stability of the metarhodopsin species (*45*), it seems likely that at room temperature the metarhodopsin species readily decays to opsin and free retinal. Our results further suggest that the metarhodopsin is actually composed of two spectrally identical species that decay at different rates. Crayfish rhodopsin exhibits two spectrally distinct forms when isolated in digitonin micelles and they form metarhodopsins with different λ_{max} (*65*). This behavior has been attributed to the detergent environment (*67*). Further work on *Rh1-1D4* will be necessary to determine how the lipid/detergent environment affects the metarhodopsin stability.

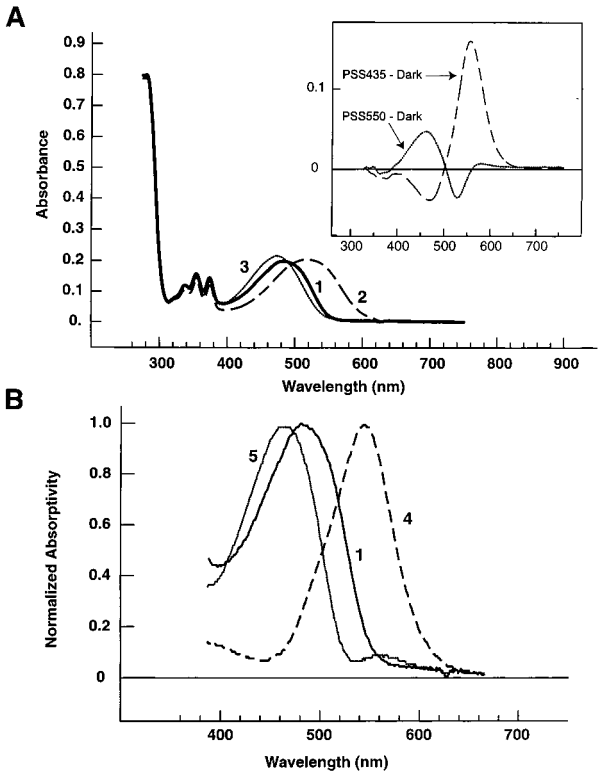

FIGURE 4: Spectroscopy and photoconversion of *Rh1-1D4* rhodopsin at 70 K. (A) Dark-adapted *Rh1-1D4* rhodopsin undergoes a red shift in the absorption maximum when cooled to 70 K (curve 1, λ_{max} = 486 nm)). Upon illumination with 435 nm light, a bathochromic photostationary state (PSS435) is generated (curve 2). The sample was then illuminated with 550 nm light (PSS550) to generate a blue-shifted photostationary state (curve 3). (Inset) Difference spectra of PSS435 minus the original pigment (dashed line) and PSS550 minus the original pigment (dotted curve) are shown. (B) The PSS435 − dark difference spectrum was used to generate an approximate bathorhodopsin spectrum (curve 4, λ_{max} = 545 nm). The PSS550 − dark difference spectrum was used to calculate an approximate isorhodopsin spectrum (curve 5, λ_{max} = 462 nm). The original *Rh1-1D4* rhodopsin pigment is shown (curve 1) for comparison.

Cryogenic Spectroscopy and Photochemistry of Rh1. To compare the properties of *Drosophila* batho-*Rh1-1D4* with the bathointermediates of the vertebrate opsins, *Rh1-1D4* was studied at low temperatures. The pH of the samples was 6.6, well below the reported metarhodopsin Schiff base pK_a of ~8.5 in mixed micelles (*45*). Under these conditions, the majority of the metarhodopsin should be protonated. An opsin sample was cooled to 70 K and allowed to thermally equilibrate for 1 h before the spectrum was recorded (Figure 4A, curve 1). At 4 °C, *Rh1-1D4* has an absorption maximum of 474 nm that shifts to 486 nm when the pigment is cooled to 70 K (see Table 2). This red shift in the absorption maximum when cooled to 70 K is also observed in some other vertebrate opsins (*68*−*71*). Upon illumination at 70 K, the opsin absorption spectrum broadens and the maximum shifts to longer wavelengths. Continuous illumination with 435 nm light, until no further spectral changes were found, produced a photostationary state termed PSS435 (Figure 4A, curve 2). The difference spectrum, PSS435 minus the original dark species, is shown (Figure 4A, inset). To investigate the reversibility of the low-temperature intermediates, PSS435

Table 2: Spectroscopic Properties of *Drosophila Rh1-1D4* Rhodopsin

	T (K)	λ_{max}[a] (nm)	$\Delta\nu_{fwhm}$[a] (cm^{-1})
WT	277	474	4700
meta[b]	277	572	3300
WT	70	484	4580
PSS435	70	516	4930
PSS550	70	473	4290
batho-*Rh1-1D4*	70	545	
iso-*Rh1-1D4*	70	462	

[a] Data for WT, PSS435, and PSS550 at 70 K were obtained by using a log-normal fit (see discussion in (ref *77*). The skewness parameters obtained from the fit are as follows: WT ($\rho = 1.751$), PSS435 ($\rho = 1.625$), and PSS550 ($\rho = 1.497$). [b] Metarhodopsin (20 °C, pH 6.6) has $\tau_1 = 280$ s and $\tau_2 = 2700$ s.

was illuminated with 550 nm light to produce a photostationary state, PSS550. Although illumination of PSS435 reversed the bathointermediate of the pigment back to a state similar to the unilluminated state (Figure 4A, curve 3), the λ_{max}, 474 nm, was blue-shifted compared to the dark state, 486 nm. The absorption difference spectrum (PSS550 minus the original dark spectrum) illustrates this shift clearly (Figure 4A, inset).

At 70 K, the retinal binding site of rhodopsin and other vertebrate opsins can accommodate 11-*cis*-retinal (the initial dark state) along with *all-trans*-retinal (the primary photoproduct) and 9-*cis*-retinal (isorhodopsin). By illuminating vertebrate rhodopsin with blue light relative to the absorption maximum, the *all-trans*-retinal species is favored. However, 100% conversion is never achieved since the absorption spectra of the 11-*cis*-, 9-*cis*-, and all-*trans*-retinal species overlap, permitting photoconversion among all three. The low-temperature photostationary state (PSS458) formed in bovine rhodopsin contains approximately ~60% of the pigment as the red-shifted, primary intermediate bathorhodopsin with an *all-trans*-retinal chromophore (*48*, *72*, *73*). If vertebrate rhodopsin is illuminated at low temperature with light on the red side of the absorption maximum (565 nm), approximately ~90% of the pigment in the PSS565 mixture contains 9-*cis*-retinal (*48*, *72*, *73*). The presence of 9-*cis*-retinal is observable by a blue shift in the absorption maximum in the reverse photostationary state.

Drosophila Rh1-1D4 behaves like vertebrate opsins at cryogenic temperatures. When the pigment is exposed to low temperature, the absorption maximum shifts from 474 to 486 nm (cf. bovine rhodopsin from 500 to 505 nm). When the protein is illuminated with blue light relative to the absorption peak (435 nm), a bathochromic photostationary state is formed. Red light relative to the absorption maximum (550 nm) then induces a blue shift relative to the initial absorption maximum. Therefore, PSS435 should contain mostly *all-trans*-, and 11-*cis*-retinal with a small amount of 9-*cis*-retinal. By taking the PSS435 minus initial state difference spectrum (Figure 4A, inset) and incrementally adding back the initial spectrum (11-*cis*-retinal opsin) until the resulting curve fits a log normal equation, an approximate batho-*Rh1-1D4* spectrum was generated, with a $\lambda_{max} \sim 545$ nm (Figure 4B, curve 4). In a similar fashion, the iso-*Rh1-1D4* spectrum, i.e. containing a 9-cis chromophore, was estimated to have a $\lambda_{max} \sim 462$ nm (Figure 4B, curve 5) by adding about 30% of the initial spectrum back to the PSS550 minus initial dark state difference spectrum (Figure 4A, inset).

The cryogenic batho − product difference spectra of *Drosophila Rh1-1D4* rhodopsin (PSS435 minus dark from Figure 4A, inset) and selected vertebrate visual pigments were normalized (the absorptivity maxima set to unity) and then integrated under the positive and negative going bands:

$$I_{pos} = \int_{\tilde{\nu}_1}^{\tilde{\nu}_2} \mathrm{Norm}[\mathrm{PSS}_{\lambda_B}(\tilde{\nu}) - R(\tilde{\nu})]\, d\tilde{\nu} \quad (1)$$

$$I_{neg} = \int_{\tilde{\nu}_2}^{\tilde{\nu}_3} \mathrm{Norm}[\mathrm{PSS}_{\lambda_B}(\tilde{\nu}) - R(\tilde{\nu})]\, d\tilde{\nu} \quad (2)$$

where $\mathrm{PSS}_{\lambda_B}(\tilde{\nu})$ is the photostationary state induced by excitation at λ_B, $R(\bar{\nu})$ is the spectrum of the initial (11-cis chromophore) state, Norm[x] represents the ($\lambda_{max} \rightarrow 1$) normalization function, and the frequency values $\bar{\nu}_1$, $\bar{\nu}_2$, and $\bar{\nu}_3$ are where the absorption equals 0 at the red edge of the difference spectrum, the crossing point from the positive to negative portion of the difference spectrum, and the blue edge of the difference spectrum, respectively (see ref *48* for a discussion). The absolute values of the positive and negative integrals are plotted as a function of the difference spectrum frequency maxima in the lower panel of Figure 5. The upper panel of this figure shows the shift in the frequency of the absorption maximum between the (all-trans) bathophotoproduct and the (11-cis chromophore) initial state. We have added additional pigments in both graphs for comparative purposes. By normalizing the difference spectra, the band integrals are independent of the primary event quantum efficiency. These integrals are sensitive to the changes in both the frequency and shape of the initial and subsequent absorption spectra as well as the change in the oscillator strength of the λ_{max} band that accompanies the primary photochemical event.

The trends observed in Figure 5 provide a window on the mechanism of spectral tuning in these pigments. One of the questions to be answered is whether the retinal Schiff base linkage has a counterion in the invertebrate pigments. The position equivalent to the Asp or Glu counterion in the vertebrate pigments is occupied by a Tyr in most of the invertebrate opsins. The observation that the *Drosophila Rh1-1D4* opsin integral trends shown in Figure 5 are systematically identical to those observed for the vertebrate opsins provides strong evidence in support of a conserved mechanism for spectral tuning both within and across both classes. We suggest that *Rh1-1D4* rhodopsin most likely has a protonated Schiff base with a single negatively charged counterion regulating the spectroscopic and photochemical properties of the pigment. Previous studies have shown the retinal Schiff base is protonated in invertebrate pigments (*14*−*16*). The data presented in Figure 5 provide evidence that the 11-cis protonated Schiff base chromophore is mediated by a single, negatively charged counterion in close proximity to the conjugated π-system of the chromophore. Otherwise, we would expect the *Rh1-1D4* integrals to not follow the trend lines established by the other pigments with binding sites that fit this description. We note that for a visual pigment to display optical characteristics that follow these trends requires two characteristics of the binding site: a protonated chromophore and a single, negatively charged counterion near the chromophore. If protonation were the only requirement, bacteriorhodopsin would fall on the trend line. It does not, and this is due in part to the complex

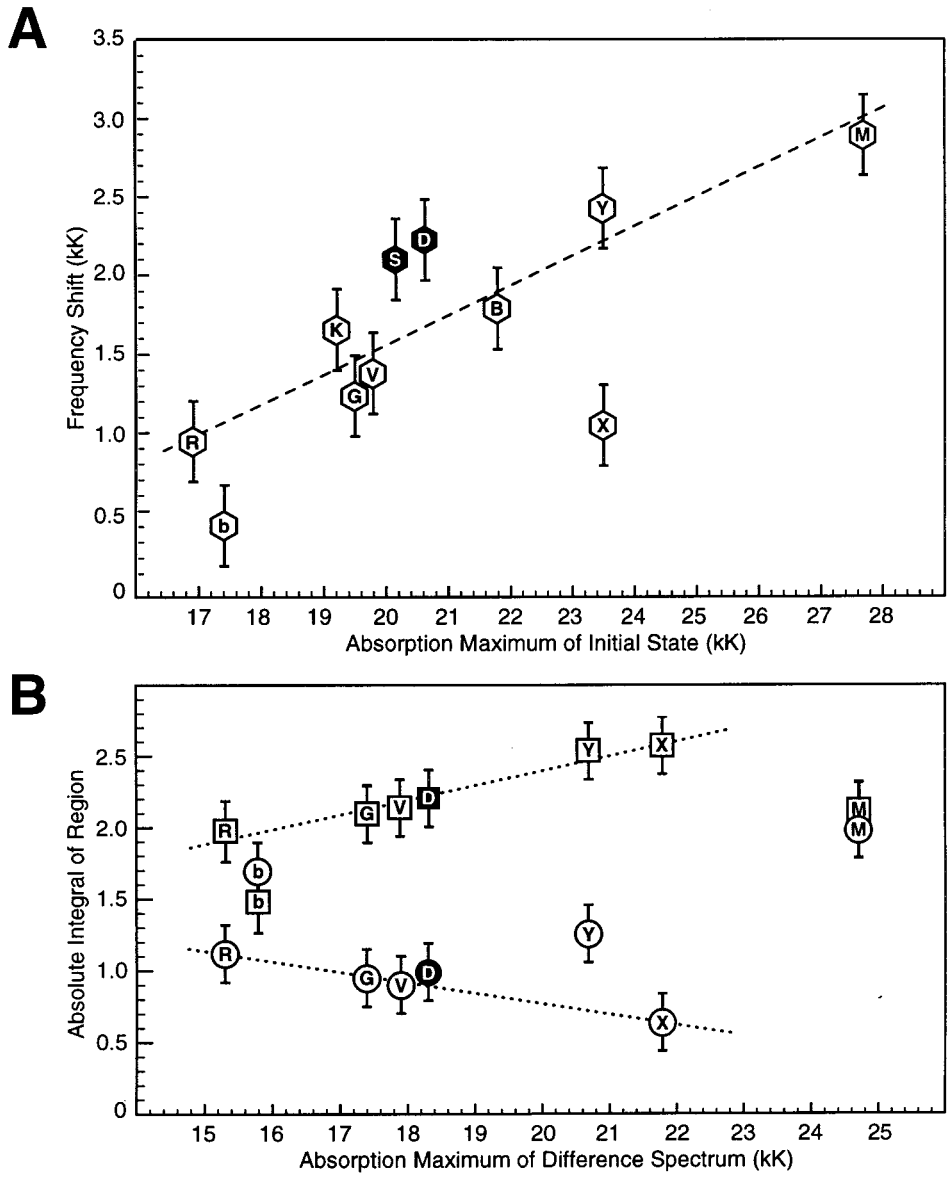

FIGURE 5: (A) Frequency shift associated with formation of the bathophotoproduct (1 kK = 1000 cm^{-1}) versus the absorption maximum of the initial (11-cis) protein. (B) Integrals of the positive and negative bands in the bathochromic difference spectra of selected pigments plotted versus the wavenumber of the peak absorptivity difference [I_{pos} (eq 2) in squares, $-I_{neg}$ (eq 3) in circles]. The letters indicate the pigment and, where relevant, conditions (the invertebrate pigments are shaded darker): b = bacteriorhodopsin (light-adapted), R = chicken red cone opsin (*78*), K = gecko green cone opsin (P521) (*69*), G = chicken green cone opsin (*70*), V = bovine rhodopsin (*48*), S = squid rhodopsin (*68*), D = *Drosophila Rh1-1D4* rhodopsin (this study), B = chicken blue cone opsin (*71*), Y = *X. laevis* violet cone opsin at 70 K (*48*), X = *X. laevis* violet cone opsin at 30 K (*48*), and M = mouse UV cone opsin (*48*).

(quadrupole-like) counterion environment of this light-transducing protein (*74*). An alternative example is the UV cone pigment of the mouse, which appears to have an unprotonated chromophore (*48*) and displays integral values that are shifted significantly from the trend lines (see Figure 5). The photophysical origins of these trends can be traced to the influence of binding site electrostatics on the transition energy and oscillator strength of the low-lying strongly allowed ^1B_u-like π,π^* state (*7*). A more detailed discussion of these issues can be found in ref *48*. The question that remains to be resolved is what is the counterion.

Potential amino acid counterions include Tyr (at the equivalent vertebrate counterion position), an Asp that is conserved among invertebrates in helix 2 (D96 in *Drosophila* Rh1), or a conserved Asp/Glu on the cytoplasmic face of helix 3. Several lines of evidence suggest that the Tyr residue is protonated and thus cannot be the counterion (*27*, *75*). To maintain a neutral binding site, a previously unidentified amino acid residue or anion must serve as a counterion to the Schiff base. Ebrey and co-workers (*27*, *76*) have shown that various anions do not affect the absorption maximum of octopus rhodopsin, thus suggesting that a solvent anion cannot serve as a counterion. Further investigations are required to identify the putative invertebrate counterion and the molecular origins of bistability in the invertebrate retina.

CONCLUSIONS

In this paper, we presented methods for isolating and purifying invertebrate visual pigments in sufficient quantities for traditional spectroscopic and biochemical characterization. We also presented low-temperature (70 K) spectroscopic studies of the most abundant opsin from the *Drosophila* retina, *Rh1* rhodopsin. By comparing the photochemical and spectroscopic properties of this pigment with other vertebrate

pigments, we conclude that the binding site of this protein is electrostatically similar to bovine rhodopsin and most likely has a single counterion generating a neutral chromophore binding site.

ACKNOWLEDGMENT

We thank W.-H. Chou for performing the immunohistochemistry and confocal microscopy and P. Dolph for antibodies against arrestins 1 and 2.

REFERENCES

1. Wald, G. (1968) *Science 162*, 230−239.
2. Hargrave, P. A., and McDowell, J. H. (1992) *Int. Rev. Cytol.* 49−97.
3. Scott, K., Becker, A., Sun, Y., Hardy, R., and Zuker, C. (1995) *Neuron 15*, 919−927.
4. Zhukovsky, E. A., and Oprian, D. D. (1989) *Science 246*, 928−30.
5. Sakmar, T. P., Franke, R. R., and Khorana, H. G. (1989) *Proc. Natl. Acad. Sci. U.S.A. 86*, 8309−13.
6. Nathans, J. (1990) *Biochemistry 29*, 9746−52.
7. Birge, R. R., Murray, L. P., Pierce, B. M., Akita, H., Balogh-Nair, V., Findsen, L. A., and Nakanishi, K. (1985) *Proc. Natl. Acad. Sci. U.S.A. 82*, 4117−21.
8. Hamdorf, K. (1979) in *Handbook of sensory physiology* (Autrum, H., Ed.) pp 145−224, Springer, Berlin.
9. Hamdorf, K., Paulsen, R., and Schwemer, J. (1973) in *Biochemistry and physiology of visual pigments* (Langer, H., Ed.) pp 155−166, Springer, Berlin.
10. Hillman, P., Hochstein, S., and Minke, B. (1983) *Physiol. Rev. 63*, 668−772.
11. Schwemer, J. (1984) *J. Comput. Physiol. A 154*, 535−547.
12. Gärtner, W., and Towner, P. (1995) *Photochem. Photobiol. 62*, 1−16.
13. Hashimoto, S., Takeuchi, H., Nakagawa, M., and Tsuda, M. (1996) *FEBS Lett. 398*, 239−42.
14. Kitagawa, T., and Maeda, A. (1989) *Photochem. Photobiol. 50*, 883−94.
15. Pande, C., Pande, A., Yue, K. T., Callender, R., Ebrey, T. G., and Tsuda, M. (1987) *Biochemistry 26*, 4941−7.
16. Pande, A. J., Callender, R. H., Ebrey, T. G., and Tsuda, M. (1984) *Biophys. J. 45*, 573−6.
17. Suzuki, T., Uji, K., and Kito, Y. (1976) *Biochim. Biophys. Acta 428*, 321−338.
18. Kobayashi, T., and Nagakura, S. (1982) in *Methods in Enzymology* (Colowick, S. P., and Kaplan, N. O., Eds.) Vol. 81, pp 368−373, Academic Press, New York.
19. Tsuda, M. (1979) *Biochim. Biophys. Acta 545*, 537−546.
20. Ebina, Y., Nagasawa, N., and Tsukahara, Y. (1975) *Jpn. J. Physiol. 25*, 217−226.
21. Naito, T., Nashima-Hayma, K., Ohtsu, K., and Kito, Y. (1981) *Vision Res. 21*, 935−941.
22. Koutalos, Y., Ebrey, T. G., Tsuda, M., Odashima, K., Lien, T., Park, M. H., Shimizu, N., Derguini, F., Nakanishi, K., Gilson, H. R., and Honig, B. (1989) *Biochemistry 28*, 2732−2739.
23. Tokunga, F., Shichida, Y., and Yoshizawa, T. (1975) *FEBS Lett. 55*, 229−232.
24. Shichida, Y., Yoshizawa, T., Kobayashi, T., Ohtani, H., and Nagakura, S. (1977) *FEBS Lett. 80*, 214−216.
25. Yoshizawa, T., Shichida, Y., and Matuoka, S. (1984) *Vision Res. 24*, 1455−1463.
26. Longstaff, C., Calhoon, R. D., and Rando, R. R. (1986) *Proc. Natl. Acad. Sci. U.S.A. 83*, 4209−4213.
27. Nakagawa, M., Iwasa, T., Kikkawa, S., Tsuda, M., and Ebrey, T. G. (1999) *Proc. Natl. Acad. Sci. U.S.A. 96*, 6189−6192.
28. Oprian, D., Molday, R., Kaufman, R., and Khorana, G. (1987) *Proc. Natl. Acad. Sci. U.S.A. 84*, 8874−8879.
29. Ostroy, S. E., Wilson, M., and Pak, W. L. (1974) *Biochem. Biophys. Res. Commun. 59*, 960−966.
30. Ostroy, S. E. (1978) *J. Gen. Physiol. 72*, 717−732.
31. Salcedo, E., Huber, A., Henrich, S., Chadwell, L. V., Chou, W. H., Paulsen, R., and Britt, S. G. (1999) *J. Neurosci. 19*, 10716−26.
32. Tanimura, T., Isono, K., and Tsukahara, Y. (1986) *Photochem. Photobiol. 43*, 225−228.
33. Vogt, K., and Kirschfeld, K. (1984) *Naturwissenschaften 71*, 211−213.
34. Zuker, C. S., Cowman, A. F., and Rubin, G. M. (1985) *Cell 40*, 851−8.
35. O'Tousa, J. E., Baehr, W., Martin, R. L., Hirsh, J., Pak, W. L., and Applebury, M. L. (1985) *Cell 40*, 839−850.
36. Nathans, J., and Hogness, D. S. (1983) *Cell 34*, 807−814.
37. Molday, R. S., and MacKenzie, D. (1983) *Biochemistry 22*, 653−660.
38. Chou, W. H., Hall, K. J., Wilson, D. B., Wideman, C. L., Townson, S. M., Chadwell, L. V., and Britt, S. G. (1996) *Neuron 17*, 1101−15.
39. Karess, R. E., and Rubin, G. M. (1984) *Cell 38*, 135−146.
40. Townson, S. M., Chang, B. S., Salcedo, E., Chadwell, L. V., Pierce, N. E., and Britt, S. G. (1998) *J. Neurosci. 18*, 2412−2422.
41. Franceschini, N. (1985) *Neurosci. Res. Suppl. 2S*, 17−49.
42. Franceschini, N. (1979) *Invest. Opthalmol. [Suppl] 5*, 1.
43. Corripio, A. B. (1990) In *Tuning of Industrial Control Systems*, Instrument Society of America, Research Triangle Park, NC.
44. Kiselev, A., and Subramaniam, S. (1994) *Science 266*, 1369−1373.
45. Kiselev, A., and Subramaniam, S. (1996) *Biochemistry 35*, 1848−1855.
46. Starace, D. M., and Knox, B. E. (1998) *Exp. Eye Res. 67*, 209−220.
47. Dolph, P. J., Ranganathan, R., Colley, N. J., Hardy, R. W., Socolich, M., and Zuker, C. S. (1993) *Science 260*, 1910−1916.
48. Vought, B. W., Dukkipatti, A., Max, M., Knox, B. E., and Birge, R. R. (1999) *Biochemistry 38*, 11287−11297.
49. Feiler, R., Bjornson, R., Kirschfeld, K., Mismer, D., Rubin, G. M., Smith, D. P., Socolich, M., and Zuker, C. S. (1992) *J. Neurosci. 12*, 3862−3868.
50. Feiler, R., Harris, W. A., Kirschfeld, K., Wehrhahn, C., and Zuker, C. S. (1988) *Nature 333*, 737−741.
51. Britt, S. G., Feiler, R., Kirschfeld, K., and Zuker, C. S. (1993) *Neuron 11*, 29−39.
52. Kirschfeld, K., and Franceschini, N. (1977) *Nature 269*, 386-390.
53. Kirschfeld, K., and Franceschini, N. (1977) *Biophys. Struct. Mech. 3*, 191−194.
54. Kiselev, A., and Subramaniam, S. (1997) *Biochemistry 36*, 2188−2196.
55. Seki, T., and Vogt, K. (1998) *Comp. Biochem. Physiol. 119B*, 53−64.
56. Schreckenbach, T., Walckoff, B., and Oesterhelt, D. (1977) *Eur. J. Biochem. 76*, 499−511.
57. Ong, D. E. (1985) *J. Biol. Chem. 259*, 1476−1482.
58. Oroshnik, W., Karmas, G., and Mebane, A. (1952) *J. Am. Chem. Soc. 74*, 295−301.
59. Zechmeister, L. (1962) *Cis−trans isomeric carotenoids vitamins A and arylpolyenes*, Academic Press, New York.
60. Schwemer, J., and Langer, H. (1982) in *Methods in Enzymology* (Packer, L., Ed.) Vol. 81, pp 182−190, Academic Press, New York.
61. Hong, K., and Hubbell, W. (1973) *Biochemistry 12*, 4517−23.
62. Sakamoto, T., and Khorana, H. G. (1995) *Proc. Natl. Acad. Sci. U.S.A. 92*, 249−53.
63. Gibson, N., and Brown, M. (1991) *Photochem. Photobiol. 54*, 985−92.
64. Franke, R. R., Sakmar, T. P., Graham, R. M., and Khorana, H. G. (1992) *J. Biol. Chem. 267*, 14767−74.
65. Larrivee, D., and Goldsmith, T. H. (1982) *Vision Res. 22*, 727−37.
66. Bennett, R. R., and Brown, P. K. (1985) *Vision Res. 25*, 1771−81.

67. Zeiger, J., and Goldsmith, T. H. (1994) *Vision Res. 34*, 2679−88.
68. Yoshizawa, T., and Shichida, Y. (1982) in *Methods in Enzymology*, (Packer, L., Ed.) Vol. 81, pp 333−354, Academic Press, Inc., New York.
69. Kojima, D., Imai, H., Okano, T., Fukada, Y., Crescitelli, F., Yoshizawa, T., and Shichida, Y. (1995) *Biochemistry 34*, 1096−1106.
70. Imai, H., Imamoto, Y., Yoshizawa, T., and Shichida, Y. (1995) *Biochemistry 34*, 10525−10531.
71. Imai, H., Terakita, A., Tachibanaki, S., Imamoto, Y., Yoshizawa, T., and Shichida, Y. (1997) *Biochemistry 36*, 12773−12779.
72. Suzuki, T., and Callender, R. H. (1981) *Biophys. J. 34*, 261−265.
73. Schick, G. A., Cooper, T. M., Holloway, R. A., Murray, L. P., and Birge, R. R. (1987) *Biochemistry 26*, 2556−2562.
74. Kusnetzow, A., Singh, D. L., Martin, C. H., Barani, I., and Birge, R. R. (1999) *Biophys. J. 76*, 2370−2389.
75. Hashimoto, S., Takeuchi, H., Nakagawa, M., and Tsuda, M. (1996) *FEBS Lett. 398*, 239−242.
76. Koutalos, Y., Ebrey, T. G., Gilson, H. R., and Honig, B. (1990) *Biophys. J. 58*, 493−501.
77. Birge, R. R. (1990) *Biochim. Biophys. Acta 1016*, 293−327.
78. Imamoto, Y., Kandori, H., Okano, T., Fukada, Y., Shichida, Y., and Yoshizawa, T. (1989) *Biochemistry 28*, 9412−9416.

BI001135K